

Behaviour of earth's crust due to topographic loads derived by inverse and direct isostasy

Hussein A. Abd-Elmotaal *

Civil Engineering Department, Faculty of Engineering, Minia University, Minia, Egypt

Received 2 January 2013; accepted 25 December 2013

Available online 12 February 2014

KEYWORDS

Inverse problems;
Isostasy;
Loading theory;
Response function;
Density anomaly

Abstract The behaviour of the earth's crust due to topographic loads can be derived by either inverse or direct approach. As for the inverse approach, it is postulated that the density anomaly is proportional to the earth's radius vector so that it is linearly related to topography by a convolution of the topography and an isotropic kernel function. Accordingly, one can prove that the attraction of the compensating masses is also a convolution of the topography and an isotropic isostatic response function. Such an isostatic response function can be determined by deconvolution. This paper gives the derivation of such a deconvolution by means of spherical harmonics. A practical determination of the isotropic isostatic response function needs the harmonic analysis of both the topography and the attraction of the compensating masses. Applying the principle of inverse isostasy, by which we aim to achieve zero isostatic anomalies, then the attraction of the compensating masses equals the Bouguer anomalies with an opposite sign. The harmonic analysis of the Bouguer anomalies is thus a combination of the harmonic analysis of the topographic potential and the already existing global reference models. As for the direct approach, consider that the earth's crust is an infinite thin plate subject to topographic loads. The solution of such a bent plate represents the displacement of the earth's crust due to topographic loads. The paper illustrates that the exact solution of the bent plate is given by the Kelvin function $\text{kei } x$. A practical application has been carried out for both approaches using EGM96 and GPM98CR geopotential earth models as well as TUG87 and TBASE digital height models. The results show that the estimated isotropic isostatic response functions derived by the inverse approach behave similarly as that given by direct approach represented by the Kelvin function $\text{kei } x$.

© 2014 Production and hosting by Elsevier B.V. on behalf of National Research Institute of Astronomy and Geophysics.

* Tel.: +20 1225538880.

E-mail address: abdelmotaal@lycos.com

Peer review under responsibility of National Research Institute of Astronomy and Geophysics.



Production and hosting by Elsevier

1. Introduction

The estimation of the behaviour of the earth's crust due to the topographic loads is a traditional subject in geodynamics and has been investigated by many scholars. Several isostatic models have been postulated in the past.

Pratt–Hayford isostatic model assumes constant level of compensation and the topography is being compensated by

variable density contrast in a local sense. Airy–Heiskanen isostatic model assumes that the topography is floating on a denser substratum (the mantle) so that the higher it is, the deeper it sinks. Thus, here the level of compensation is variable, while the density anomaly is constant. Again, Airy–Heiskanen model assumes free mobility of the topographic elements and their compensating elements, i.e., it works in a local sense (Heiskanen and Moritz, 1967, pp. 133–137).

Veneing Meinesz has introduced regional, instead of local, floating isostatic model (Vening Meinesz, 1940). In the framework of the floating regional isostatic hypothesis, Abd-Elmotaal (1993) has given the exact bending curve of the earth's crust subject to the topographic loads.

All the models introduced above may belong to the so-called *direct models*. Another way to estimate the behaviour of the earth's crust due to the topographic loads, which may be called *inverse models*, is given by a postulation of the relation of the density anomaly and the topography.

We start with the assumption that the density anomaly $\Delta\rho$ is linearly related to the topography h by a convolution of the topography and an isotropic kernel function K , i.e.,

$$\Delta\rho(r', \theta', \lambda') = \iint_{\sigma} h(\theta'', \lambda'') K(r', \psi) d\sigma, \quad (1)$$

or symbolically

$$\Delta\rho(r', \theta', \lambda') = h(\theta'', \lambda'') * K(r', \psi), \quad (2)$$

where $*$ stands for the spatial convolution. This assumption was given first by Dorman and Lewis (1970). Accordingly, one can prove that the attraction of the compensating masses is also a convolution of the topography and an isotropic isostatic response function. Such an isostatic response function can be determined by deconvolution.

This paper gives the derivation of the isostatic response function in terms of spherical harmonics by a deconvolution of the vertical derivative of the isostatic potential. A practical computation of the isotropic isostatic response function has been carried out using EGM96 model (complete to degree and order 360) and GPM98CR (complete to degree and order 540) representing the geopotential earth model. TUG87 (30' \times 30' resolution) and TBASE (20' \times 20' and 30' \times 30' resolutions) digital height models have been used for computing the harmonic coefficients of the topography and of the topographic potential. A broad comparison of the isostatic response functions estimated within this investigation has been made. These estimated isostatic response functions are also compared with the exact solution of the earth's crust bent by the topographic loads expressed by the Kelvin function $\text{kei } x$. It should be noted that related numerical results may be found, e.g., in Lewis and Dorman (1970), Bechtel et al. (1987), and Hein et al. (1989).

2. Isostatic response function in terms of spherical harmonics

As stated earlier, postulating that the density anomaly $\Delta\rho$ is given by a convolution of the topography and an isotropic kernel function, one can derive that the attraction of the compensating masses A_C is also a convolution of the topography h and an isotropic isostatic response function $F(\psi)$ (Dorman and Lewis, 1970)

$$A_C(R, \theta, \lambda) = \iint_{\sigma} h(\theta', \lambda') F(\psi) d\sigma, \quad (3)$$

ψ denotes the spherical distance between the computational point (θ, λ) and the running point (θ', λ') , given by

$$\cos \psi = \cos \theta \cos \theta' + \sin \theta \sin \theta' \cos(\lambda' - \lambda). \quad (4)$$

where θ is the co-latitude and λ denotes the longitude.

Given the attraction of the compensating masses A_C and the topographic height h , the isostatic response function F can be determined by deconvolution of (3). We confine ourselves to the global problem, which can be solved by means of spherical harmonics.

Let us expand the three components of (3)

$$A_C(R, \theta, \lambda) = \sum_{n=0}^{\infty} \sum_{m=-n}^n A_{nm} Y_{nm}(\theta, \lambda), \quad (5)$$

$$h(\theta, \lambda) = \sum_{n=0}^{\infty} \sum_{m=-n}^n H_{nm} Y_{nm}(\theta, \lambda), \quad (6)$$

$$F(\psi) = \sum_{n=0}^{\infty} F_n P_n(\cos \psi), \quad (7)$$

where $P_n(\cos \psi)$ stands for the standard Legendre polynomial and the base functions Y_{nm} are given by Moritz (1990, p. 195)

$$Y_{nm}(\theta, \lambda) = P_{nm}(\cos \theta) \begin{cases} \cos m\lambda, & m = 0, 1, 2, \dots, n, \\ \sin m\lambda, & m = -1, -2, \dots, -n, \end{cases} \quad (8)$$

where $P_{nm}(\cos \theta)$ are the standard Legendre functions. Since F depends only on ψ , its expansion is purely zonal, cf. (7).

Substituting F from (7) into (3) gives

$$A_C(R, \theta, \lambda) = \sum_{n=0}^{\infty} F_n \iint_{\sigma} h(\theta', \lambda') P_n(\cos \psi) d\sigma. \quad (9)$$

Now by using the well-known integral formula (Heiskanen and Moritz, 1967, Eq. 1–71), one can write

$$A_C(R, \theta, \lambda) = 4\pi \sum_{n=0}^{\infty} \frac{F_n}{2n+1} H_n(\theta, \lambda). \quad (10)$$

We express the Laplace harmonic $H_n(\theta, \lambda)$ of the topography h in terms of the base functions Y_{nm}

$$H_n(\theta, \lambda) = \sum_{m=-n}^n H_{nm} Y_{nm}(\theta, \lambda). \quad (11)$$

Thus A_C is given by inserting (11) into (10)

$$A_C(R, \theta, \lambda) = 4\pi \sum_{n=0}^{\infty} \sum_{m=-n}^n \frac{F_n}{2n+1} H_{nm} Y_{nm}(\theta, \lambda). \quad (12)$$

Comparing (5) with (12) gives immediately

$$A_{nm} = \frac{4\pi}{2n+1} F_n H_{nm}. \quad (13)$$

Eq. (13) is the so-called *spherical convolution theorem* given by Moritz (1990, p. 251). Eq. (13) can be written for F_n as

$$F_n = \frac{2n+1}{4\pi} \frac{A_{nm}}{H_{nm}}, \quad (14)$$

which is *independent* of the order m . This condition should be satisfied by the topography h and the attraction of the compensating masses A_C if the assumption of isotropy is justified. Finally, the isostatic response function is given by (7) with (14).

3. Computational aspects

Eq. (14) computes F_n as a ratio of the conventional harmonic coefficients of the attraction of the compensating masses A_{nm} and of the topography H_{nm} . The conventional harmonic coefficients are related to the fully normalized ones by, e.g., (Heiskanen and Moritz, 1967, p. 32)

$$\begin{aligned}\bar{A}_{n0} &= \frac{A_{n0}}{\sqrt{2n+1}}, \\ \bar{A}_{nm} &= \sqrt{\frac{1}{2(2n+1)}} \frac{(n+m)!}{(n-m)!} A_{nm} (m \neq 0).\end{aligned}\quad (15)$$

Replacing the conventional harmonic coefficients by the fully normalized ones, the *constant* factors in the nominator and dominator of (14) will cancel, and F_n will be given by

$$F_n = \frac{2n+1}{4\pi} \frac{\bar{A}_{nm}}{\bar{H}_{nm}}, \quad (16)$$

where \bar{A}_{nm} and \bar{H}_{nm} are the fully normalized harmonic coefficients of the attraction of the topographic masses and of the topography, respectively.

Practical computation of F_n by (16) may face a problem of imperfect isotropy. This leads to loss of power of F_n , especially for higher degrees n , if one computes F_n by, e.g.,

$$F_n = \frac{2n+1}{4\pi} \left(\frac{1}{2n+1} \sum_{m=-n}^n \frac{\bar{A}_{nm}}{\bar{H}_{nm}} \right) = \frac{1}{4\pi} \sum_{m=-n}^n \frac{\bar{A}_{nm}}{\bar{H}_{nm}} \quad (17)$$

The expression in between the brackets represents the average of the ratio $\bar{A}_{nm}/\bar{H}_{nm}$; hence we have $2n+1$ ratios by degree. As it is already known in most practical applications in physical geodesy (e.g., empirical covariance function), perfect isotropy can hardly be occurred in practice, especially for the short wavelength spectrum. For the long wavelength spectrum, almost perfect isotropy can be achieved in practice. Hence, isotropic kernels (functions) are commonly postulated in physical geodesy with careful computational techniques to reduce the effect of imperfect isotropy. Accordingly, using the mean ratio (17) may yield to loss of power of F_n , especially for higher degrees. Alternatively, F_n may be computed by

$$F_n = \frac{2n+1}{4\pi} \frac{\bar{A}_n}{\bar{H}_n}, \quad (18)$$

where \bar{A}_n and \bar{H}_n are given by

$$\bar{A}_n = \sqrt{\sum_{m=-n}^n \bar{A}_{nm}^2}, \quad (19)$$

$$\bar{H}_n = \sqrt{\sum_{m=-n}^n \bar{H}_{nm}^2}. \quad (20)$$

The definition of \bar{A}_n and \bar{H}_n shows clearly the advantage of using (18) to save the power of F_n . Here there is *only* one ratio \bar{A}_n/\bar{H}_n per degree. Practical comparison between (17) and (18) will be given in Section 8.

The summation along n in (7) is infinite. Examining (18) shows that using a certain practical upper limit N_{max} , representing infinity, will change the values of the isostatic response function. As the ratio \bar{A}_n/\bar{H}_n is bounded (cf. Fig. 4), the main part in the expression (18) is the factor $2n+1$, which is nothing else but an equation of a straight line. Accordingly, for the

isostatic response function, the higher the upper limit, the larger are the values of the isostatic response function. Hence, no direct comparison of isostatic response functions could be made. To solve this, we define the *normalized* isostatic response function $\bar{F}(\psi)$ as

$$\bar{F}(\psi) = \frac{F(\psi)}{F(0)}, \quad (21)$$

where $F(0)$ stands for the value of the isostatic response function at the origin ($\psi = 0$). Thus, for the normalized isostatic response function, the maximum value at the origin will always be unity.

4. Inverse isostasy

A practical determination of the isotropic isostatic response function needs the harmonic analysis of both the topography \bar{H}_{nm} and the attraction of the compensating masses \bar{A}_{nm} , cf. (16). Creating compensating masses by means of an isostatic hypothesis already implies an assumption of the earth's isostatic response. Instead, one may wish to estimate a more realistic isostatic response of the earth without postulating an isostatic hypothesis. This may be achieved by employing the principle of inverse isostasy, by which we aim to have zero isostatic anomalies Δg_I , i.e.,

$$\Delta g_I \equiv 0. \quad (22)$$

The reader who may be interested in more details about inverse problems in isostasy is referred to, e.g., (Moritz, 1990, Sec. 8.3). Eq. (22) can alternatively be written in the form

$$A_C = -\Delta g_B, \quad (23)$$

where A_C stands for the attraction of the compensating masses, as before, and Δg_B stands for the Bouguer anomalies. Thus, the Bouguer anomalies will be used instead of the attraction of the compensating masses.

5. Harmonic analysis of compensating masses and topography

The Bouguer anomaly Δg_B is defined by

$$\Delta g_B = \Delta g_F - A_T, \quad (24)$$

where Δg_F stands for the free-air anomaly and A_T refers to the attraction of the topographic masses. Using (23), the attraction of the compensating masses may be written as

$$A_C = A_T - \Delta g_F. \quad (25)$$

Accordingly, applying simple harmonic analysis properties, the fully normalized harmonic coefficients (in the usual sense of physical geodesy) of the potential of the compensating masses \bar{C}_{nm} can be defined as

$$\bar{C}_{nm} = \bar{t}_{nm} - \bar{T}_{nm}, \quad (26)$$

where \bar{t}_{nm} are the fully normalized harmonic coefficients of the potential of the topographic masses and \bar{T}_{nm} are the fully normalized harmonic coefficients of the free-air disturbing potential. \bar{T}_{nm} are provided by the global geopotential earth models (e.g., EGM96). The harmonic analysis of the topographic potential \bar{t}_{nm} will be given in the next section. Finally, the fully normalized harmonic coefficients of the attraction of the compensating masses \bar{A}_{nm} (in gravity anomaly unites) is related to

the (unitless) fully normalized harmonic coefficients of the potential of the compensating masses \bar{C}_{nm} by (Heiskanen and Moritz, 1967, p. 89)

$$\bar{A}_{nm} = \frac{GM}{R^2} (n-1) \bar{C}_{nm}, \quad (27)$$

where GM is the geocentric gravitational constant and R is the mean earth's radius.

Expand the topography h in terms of fully normalized harmonic coefficients \bar{H}_{nm}

$$h(\theta, \lambda) = \sum_{n=0}^{\infty} \sum_{m=-n}^n \bar{H}_{nm} \bar{Y}_{nm}(\theta, \lambda), \quad (28)$$

where the fully normalized base functions \bar{Y}_{nm} are given by (analogous to (8))

$$\bar{Y}_{nm}(\theta, \lambda) = \bar{P}_{nm}(\cos \theta) \begin{cases} \cos m\lambda, & m = 0, 1, 2, \dots, n, \\ \sin m\lambda, & m = -1, -2, \dots, -n, \end{cases} \quad (29)$$

and $\bar{P}_{nm}(\cos \theta)$ are the fully normalized Legendre functions. The fully normalized harmonic coefficients \bar{H}_{nm} are orthogonal, and given by (ibid., p. 31)

$$\bar{H}_{nm} = \frac{1}{4\pi} \iint_{\sigma} h(\theta, \lambda) \bar{Y}_{nm}(\theta, \lambda) d\sigma. \quad (30)$$

The practical determination of the fully normalized harmonic coefficients \bar{H}_{nm} is carried out using the HRCOFITR program written by Abd-Elmotaal (2004) based on HARMIN and SSYNTH programs, written originally by Colombo (1981), in an iterative scheme to allow harmonic analysis on the ellipsoid and to achieve better accuracy.

6. Harmonic analysis of the topographic potential

The topographic potential T_T can be easily defined as the potential of all topographic masses outside the geoid and ocean water inside the geoid. The topographic potential T_T can be written as:

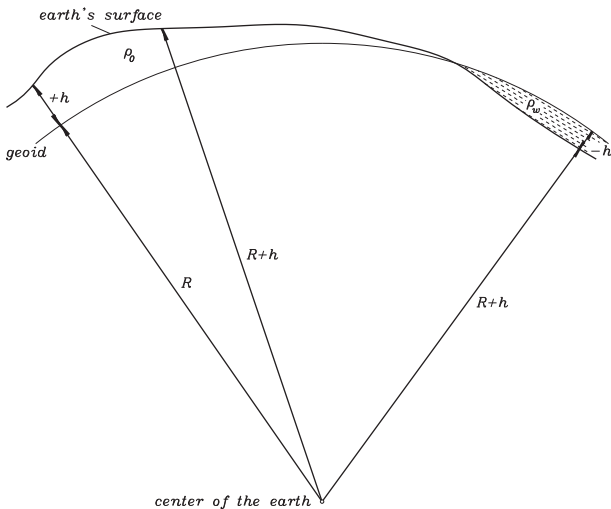


Fig. 1 Potential of the topographic masses.

$$T_T(P) = G \iiint_v \frac{\rho_Q}{\ell_{PQ}} dv_Q, \quad (31)$$

where G is Newton's gravitational constant, ρ_Q denotes the density at Q , ℓ_{PQ} is the spatial distance between P and Q and dv_Q is the volume element at Q .

It is known that T_T is harmonic outside the earth's surface and its spherical harmonic series is convergent outside a sphere completely enclosing the earth (Heiskanen and Moritz, 1967, p. 60). Outside that sphere, the convergent series representation of the reciprocal distance can be used (ibid., p. 33)

$$\frac{1}{\ell_{PQ}} = \sum_{n=0}^{\infty} \frac{r_Q^n}{r_P^{n+1}} P_n(\cos \psi_{PQ}), \quad (32)$$

where r is the modulus of the radius vector, $P_n(\cos \psi)$ is the conventional Legendre polynomial of degree n and ψ_{PQ} is the spherical distance between P and Q .

The Legendre polynomial may be expressed as (ibid., p. 33)

$$P_n(\cos \psi_{PQ}) = \frac{1}{2n+1} \sum_{m=-n}^n \bar{R}_{nm}(P) \bar{R}_{nm}(Q). \quad (33)$$

with the fully normalized spherical harmonics

$$\bar{R}_{nm}(P) = \sqrt{2^{1-\delta_{m0}} (2n+1) \frac{(n-m)!}{(n+m)!}} P_{nm}(\cos \theta_P) \begin{cases} \cos m\lambda_P & \text{for } m \leq 0 \\ \sin m\lambda_P & \text{for } m > 0 \end{cases} \quad (34)$$

with

$$\delta_{ij} = \begin{cases} 1 & \text{if } j = i \\ 0 & \text{if } j \neq i \end{cases}, \quad (35)$$

where θ is the polar distance, λ is the geodetic longitude, δ_{ij} is the Kronecker symbol and $P_{nm}(\cos \theta)$ is the Legendre function of degree n and order m . Thus the topographic potential can be represented by

$$T_T(P) = G \sum_{n=0}^{\infty} \frac{1}{(2n+1)r_P^{n+1}} \sum_{m=-n}^n \bar{R}_{nm}(P) \left[\iiint_v \rho_Q r_Q^n \bar{R}_{nm}(Q) dv_Q \right] \quad (36)$$

with

$$dv = r^2 dr d\sigma, \quad (37)$$

where $d\sigma$ is the spherical surface element.

To calculate the volume integral inside the brackets of (36), we will confine ourselves to the spherical approximation (the geoid is represented by a sphere of radius R (Sünkel, 1985); cf. Fig. 1). Then its contribution due to the topographic masses outside the geoid and ocean water inside the geoid, see Fig. 1, is

$$\iiint_v = \iiint_{r=R}^{R+h} \rho_Q r_Q^{n+2} dr_Q \bar{R}_{nm}(Q) d\sigma_Q, \quad (38)$$

where R is the radius of the mean earth's sphere and h is the topographic height (+) or ocean bottom depth (-).

The integration of (38) with respect to r is straightforward and is expressed as (Sünkel, 1985, p. 5)

$$\iiint_v = \frac{R^{n+3}}{n+3} \iint_{\sigma} \rho_Q \left[\left(1 + \frac{h_Q}{R} \right)^{n+3} - 1 \right] \bar{R}_{nm}(Q) d\sigma_Q. \quad (39)$$

Hence, the harmonic coefficients of the topographic potential \bar{t}_{nm} and the harmonic series expansion of the topographic potential can be expressed, by inserting (39) into (36), as

$$T_T(P) = \frac{GM}{r_P} \sum_{n=0}^{\infty} \left(\frac{R}{r_P}\right)^n \sum_{m=-n}^n \bar{t}_{nm} \bar{R}_{nm}(P), \quad (40)$$

where

$$\bar{t}_{nm} = \frac{R^3}{M(2n+1)(n+3)} \iint_{\sigma} \rho_Q \left[\left(1 + \frac{h_Q}{R}\right)^{n+3} - 1 \right] \bar{R}_{nm}(Q) d\sigma_Q, \quad (41)$$

where M denotes the mass of the earth, given by

$$M = \frac{4\pi R^3}{3} \rho_M, \quad (42)$$

where ρ_M denotes the mean earth's density

$$\rho_M = 5.517 \text{ g/cm}^3.$$

For the practical determination of the harmonic coefficients of the topographic potential \bar{t}_{nm} , (41) may be written as

$$\bar{t}_{nm} = \frac{3\Delta\phi\Delta\lambda}{4\pi\rho_M(2n+1)(n+3)} \sum_i^{\phi} \sum_j^{\lambda} \rho_{ij} \left[\left(1 + \frac{h_{ij}}{R}\right)^{n+3} - 1 \right] \begin{Bmatrix} \cos m\lambda_j \\ \sin m\lambda_j \end{Bmatrix} \cdot \bar{P}_{nm}(\cos\theta_i) \cos\phi_i, \quad (43)$$

where \sum denotes the summation along ϕ and λ , $\Delta\phi$ and $\Delta\lambda$ are the grid sizes of the used digital height model in the latitude and the longitude directions, respectively, and ρ is given by

$$\begin{aligned} \rho &= \rho_o & \text{for } h \geq 0, \\ \rho &= \rho_o - \rho_w & \text{for } h < 0, \end{aligned} \quad (44)$$

where ρ_o is the constant density of the topography and ρ_w is the density of the ocean's water.

7. Exact solution of the earth's crust bent by topographic load

As mentioned earlier, the behaviour of the earth's crust can also be estimated by the so-called direct approach. The direct approach deals generally with the isostatic models. Here we are going to review the most realistic regional isostatic model in the framework of the floating plate hypothesis.

Let us assume that the earth's crust (of density ρ_o) is represented by an infinite thin plate floating on a denser substratum (the mantle of density ρ_1) bent by the topographic load, Fig. 2. To get a horizontal upper surface, the dotted hollow area appearing in Fig. 2 should be filled. This represents the so-called *indirect effect*. The equation of equilibrium for that floating bent plate (taking the indirect effect into account) is

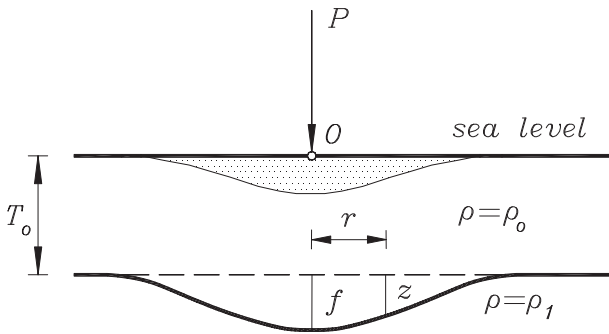


Fig. 2 Bending curve of the earth's crust due to topographic loads.

then given by Abd-Elmotaal (1993, pp. 121–122), Turcotte and Schubert (1982)

$$D\Delta^2 z = P - g(\rho_1 - \rho_o)z, \quad (45)$$

where D is the cylindrical rigidity of the plate, z is the downward displacement, g is the gravity and Δ denotes the two dimensional Laplace operator defined as

$$\Delta \equiv \frac{\partial^2}{\partial x^2} + \frac{\partial^2}{\partial y^2}. \quad (46)$$

Let us consider a point load of a unit mass to be concentrated at the origin O . Then, outside the origin O , $P = 0$. So that (45) will be reduced to

$$D\Delta^2 z = -g(\rho_1 - \rho_o)z, \quad (47)$$

or we can write it in the form

$$\Delta^2 z + l^4 z = 0 \quad (48)$$

with

$$l = \sqrt[4]{\frac{D}{g(\rho_1 - \rho_o)}}. \quad (49)$$

Eq. (49) gives the same expression for the so-called *degree of regionality* l as given by Vening Meinesz (1940, p. 5).

It can be proved that the Kelvin Function $\text{kei } x$ gives an exact solution of (48) (Abd-Elmotaal, 1993, pp. 172–173). Hence, in the sequel, the Kelvin function $\text{kei } x$ will be called the *exact solution of the earth's bending curve*.

It should be noted that an alternative solution for the spherical earth can be found in Brothie and Silvester (1969).

8. Computational results

Two digital height models have been used in this investigation. They are TUG87 (Wieser, 1987) of $30' \times 30'$ resolution and TBASE (Row and Hastings, 1995) of $20' \times 20'$ and $30' \times 30'$ resolutions. EGM96 model (Lemoine et al., 1998), complete to degree and order 360, and GPM98CR model (Wenzel, 1998), complete to degree and order 540, have been used representing the geopotential earth model.

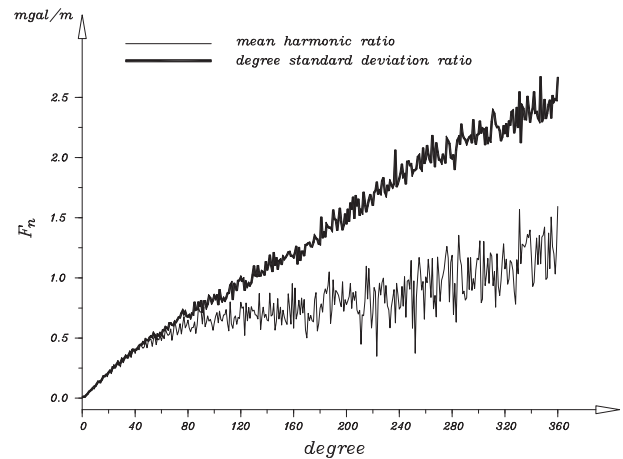


Fig. 3 F_n computed by mean harmonic ratio (17) and degree standard deviation ratio (18) using TUG87 DHM and EGM96 geopotential earth model.

Fig. 3 shows a comparison of computing F_n by (17) and (18) using TUG87 digital height model and EGM96 geopotential earth model. It shows that for the lower degrees (till around $n = 40$) both curves are nearly coincident. This reveals the perfect isotropy for long wavelength spectrum (independency of the used computational formula). For higher degrees, however, Eq. (18) saves the power of F_n with less variations between degree-to-degree values. Please refer to the appropriate discussion at Section 3.

Fig. 4 shows F_n computed by (18) using TBASE DHM ($30' \times 30'$ resolution for $N_{max} = 360$ and $20' \times 20'$ resolution for $N_{max} = 540$) and GPM98CR geopotential earth model. The behaviour of F_n shows, more or less, a linear function, which follows directly the definition of F_n (note the factor $(2n + 1)$ appearing in (16) which is an equation of a straight line). Fig. 4 shows clearly that using a higher value for N_{max} , representing infinity, will change the values of the isostatic response function F . Hence, no direct comparison of isostatic response functions could be made. To solve this, we introduced the definition of the normalized isostatic response function $\bar{F}(\psi)$ (cf. (21)).

Fig. 5 shows the normalized isostatic response functions compared to the Kelvin function $\text{kei } x$. Two normalized isostatic response functions are considered here. The first uses EGM96 geopotential earth model and TUG87 DHM with $N_{max} = 360$. The second uses GPM98CR geopotential earth model and TBASE DHM ($20' \times 20'$) with $N_{max} = 540$. For the Kelvin function $\text{kei } x$, a value of the degree of regionality l of 20 km has been chosen. The degree of regionality l is a function of the changeable physical parameters of the earth's crust (cf. (49)). Hence, an exact estimation of l is obviously hard, and usually one tries to reasonably assume it.

Fig. 5 shows that the normalized isostatic response functions and the Kelvin function $\text{kei } x$ give nearly the same values. For the Kelvin function $\text{kei } x$, the degree of regionality l may play a role of a fitting parameter. Fig. 5 shows that the isostatic behaviour of the earth's crust computed by *direct* isostasy using the most realistic isostatic model (expressed by the *exact* solution of the earth's crust subject to the topographic loads,

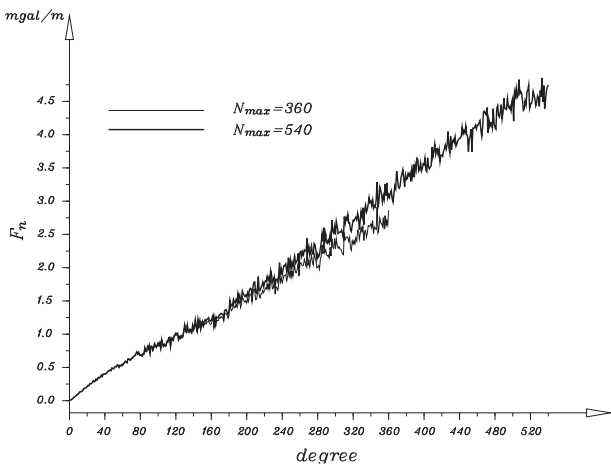


Fig. 4 F_n computed by (18) using TBASE DHM ($30' \times 30'$ resolution for $N_{max} = 360$ and $20' \times 20'$ resolution for $N_{max} = 540$) and GPM98CR geopotential earth model.

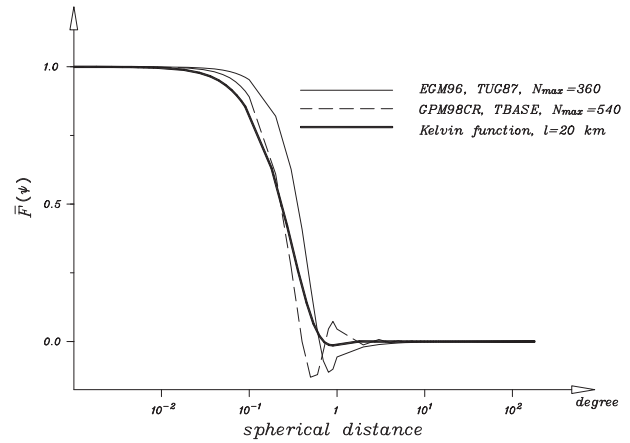


Fig. 5 Normalized isostatic response functions compared to Kelvin function $\text{kei } x$.

given by the Kelvin function $\text{kei } x$) matches the isostatic behaviour of the earth's crust derived by *inverse* isostasy.

It should be noted that using GPM98CR geopotential earth model and TBASE DHM ($30' \times 30'$ resolution) with $N_{max} = 360$ gives a normalized isostatic response function practically coincident with that using EGM96 geopotential earth model and TUG87 DHM with $N_{max} = 360$. This shows the insignificant effect of the used digital height and the geopotential earth models.

9. Conclusion

This paper gives the derivation of the isostatic response function in terms of spherical harmonics by a deconvolution of the vertical derivative of the isostatic potential. A practical determination of the isotropic isostatic response function needs the harmonic analysis of both the topography and the attraction of the compensating masses. One may try to estimate a reasonable isostatic behaviour of the earth's crust without postulating an isostatic hypothesis. This has been carried out by employing the principle of inverse isostasy, by which one tries to achieve zero isostatic anomalies. Thus, the Bouguer anomalies replace the attraction of the compensating masses. The harmonic analysis of the Bouguer anomalies is thus a combination of the harmonic analysis of the topographic potential and the already existed global (free-air) reference models.

A practical computation of the isotropic isostatic response function has been carried out using EGM96 model (complete to degree and order 360) and GPM98CR (complete to degree and order 540) representing the geopotential earth model. TUG87 ($30' \times 30'$ resolution) and TBASE ($20' \times 20'$ and $30' \times 30'$ resolutions) digital height models have been used for computing the harmonic coefficients of the topography and of the topographic potential. The results show that the normalized isostatic response functions and the Kelvin function $\text{kei } x$ give nearly the same values. This shows that the isostatic behaviour of the earth's crust computed by *direct* isostasy using the most realistic isostatic model (modified Vening Meinesz isostatic model with Kelvin function $\text{kei } x$ as the exact bending curve) matches the isostatic behaviour of the earth's crust derived by *inverse* isostasy.

References

- Abd-Elmotaal, H., 1993. Vening Meinesz moho depths: traditional, exact and approximated. *Manuscripta Geodaetica* 18, 171–181.
- Abd-Elmotaal, H., 2004. An efficient technique for harmonic analysis on a spheroid (ellipsoid and sphere). *Österreichische Zeitschrift für Vermessung & Geoinformation* 3+4, 126–135.
- Bechtel, T.D., Forsyth, D.W., Swain, C.J., 1987. Mechanisms of isostatic compensation in the vicinity of the East African Rift, Kenya. *Geophys. J. Roy. Astr. Soc.* 90, 445–465.
- Brotchie, J.F., Silvester, R., 1969. On crustal flexure. *J. Geophys. Res.* 74, 5240–5252.
- Colombo, O., 1981. In: *Numerical Methods for Harmonic Analysis on the Sphere*, Department of Geodetic Science, vol. 310. The Ohio State University, Columbus, OH.
- Dorman, L.M., Lewis, B.T.R., 1970. Experimental Isostasy: 1. Theory of the Determination of the Earth's Isostatic Response to a Concentrated Load. *J. Geophys. Res.* 75, 3357–3365.
- Hein, G.W., Eissfeller, B., Ertel, M., Hehl, K., Jacoby, W. and Czerwek, D., 1989. On Gravity Prediction Using Density and Seismic Data, Preprint, Institute of Astronomical and Physical geodesy, University FAF Munich.
- Heiskanen, W.A., Moritz, H., 1967. *Physical Geodesy*. Freeman, San Francisco.
- Lemoine, F., Kenyon, S., Factor, J., Trimmer, R., Pavlis, N., Chinn, D., Cox, C., Klosko, S., Luthcke, S., Torrence, M., Wang, Y., Williamson, R., Pavlis, E., Rapp, R., Olson, T., 1998. The Development of the Joint NASA GSFC and the National Imagery and Mapping Agency (NIMA) Geopotential Model EGM96, NASA/TP-1998-206861. NASA Goddard Space Flight Center, Maryland.
- Lewis, B.T.R., Dorman, L.M., 1970. Experimental isostasy: 2. An isostatic model for the USA derived from gravity and topographic data. *J. Geophys. Res.* 75, 3367–3386.
- Moritz, H., 1990. *The Figure of the Earths: Theoretical Geodesy and the Earth's Interior*. Wichmann, Karlsruhe.
- Row III, L.W., Hastings, D., 1995. Terrain Base Global Terrain Model. National Geophysical data Center and World Data Center-A for Solid Earth Geophysics, Boulder, CO, URL: ftp://ftp.ngdc.noaa.gov/Solid_Earth/Topography/tbase_5min/tbase.txt.
- Sünkel, H., 1985. In: *An Isostatic Earth Model*, Department of Geodetic Science, vol. 367. Ohio State University, Columbus, OH.
- Turcotte, D.L., Schubert, G., 1982. *Geodynamics: Applications of Continuum Physics to Geological Problems*. John Wiley & Sons, New York.
- Vening Meinesz, F.A., 1940. Fundamental tables for regional isostatic reduction of gravity values. *Publ. Netherlands Acad. Sci. Sec. 1 DI*. 17 (3), 1–44.
- Wenzel, H.G., 1998. Ultra High Degree Geopotential Models GPM98A, B and C to Degree 1800. URL: [http://www.gik.uni-karlsruhe.de/\(sim\)wenzel/gpm98abc/gpm98abc.htm](http://www.gik.uni-karlsruhe.de/(sim)wenzel/gpm98abc/gpm98abc.htm).
- Wieser, M., 1987. The Global Digital Terrain Model TUG87. Internal report, Graz University of Technology, Graz.